DE GRUYTER DOI 10.1515/htmp-2013-0061 — High Temp. Mater. Proc. 2014; 33(4): 305–312

Jie Dang, Guo-Hua Zhang and Kuo-Chih Chou*

Phase Transitions and Morphology Evolutions during Hydrogen Reduction of MoO_3 to MoO_2

Abstract: In the present work, studies of phase transitions and morphology evolutions during hydrogen reduction of MoO_3 to MoO_2 were carried out in the temperature range from 678 to 829 K. It was found that no intermediate phase was formed and MoO_2 was the unique detectable product during the reduction at 678 K. While above 713 K, an intermediate phase of Mo_4O_{11} was formed. The formation of Mo_4O_{11} was found to obey the consecutive mechanism under the experimental condition. Regarding the morphology evolution of MoO_2 during reduction, it was found that in the temperature range from 713 to 733 K, MoO_3 was firstly reduced to large spherical or oval Mo_4O_{11} grains, then to small spherical or oval MoO_2 ones. From 793 to 829 K, most of MoO_3 grains were firstly reduced to large plate-shaped Mo_4O_{11} grains, subsequently to small plate-shaped MoO_2 ones.

Keywords: MoO_3, Mo_4O_{11}, MoO_2, formation mechanism, morphology evolutions, hydrogen reduction

PACS® (2010). 82.20.Hf

1 Introduction

The industrial production of metallic molybdenum powders is a stepwise process that begins with the reduction of MoO_3 to MoO_2 by hydrogen [1]. This step is the crucial stage in producing metallic molybdenum, for it has a great influence on the purity and morphology of produced Mo powder [2–3]. Consequently, the mechanism of hydrogen reduction of MoO_3 to MoO_2 was widely studied in the past decades of years. However, as molybdenum can be formed a number of crystalographically well defined sub-oxides (Mo_nO_{3n-1}, e.g., Mo_9O_{26}, Mo_8O_{23}, Mo_5O_{14}, and Mo_4O_{11}) [4], fierce debate prevails regarding the existence of intermediates during the reduction. The main different viewpoints are focused on whether the intermediate product Mo_4O_{11} is formed and what is its formation mechanism. In the previous studies, five candidate reduction mechanisms were proposed.

1.1 Topotactic mechanism or one-step reduction mechanism

The initially proposed mechanism was a topotactic mechanism (direct reduction of MoO_3 to MoO_2) [5–9].

$$MoO_3(s) + H_2(g) \rightarrow MoO_2(s) + H_2O(g) \qquad (1)$$

1.2 Consecutive mechanism or two-step reduction mechanism

In contrast to one-step reduction mechanism, Burch [10] was the first who suggested that Mo_4O_{11} was an intermediate product. Since then, the formation of Mo_4O_{11} has been confirmed experimentally by many investigators [3–4, 11–12], and the remaining question has been focused on the formation mechanism of Mo_4O_{11}. One of the mechanisms postulated was a consecutive mechanism one [3, 11, 13], which considered Mo_4O_{11} being an intermediate product (Eqs. (2a) and (2b)).

$$4MoO_3(s) + H_2(g) \rightarrow Mo_4O_{11}(s) + H_2O(g) \qquad (2a)$$

$$Mo_4O_{11}(s) + 3H_2(g) \rightarrow 4MoO_2(s) + 3H_2O(g) \qquad (2b)$$

Sloczynski and Bobinski [14] have developed a consecutive autocatalytic reaction (CAR) model to describe this process.

1.3 Comproportionation mechanism

Subsequent studies using in situ XAS and XRD suggested that at temperature below 698 K, the reduction of MoO_3

***Corresponding author: Kuo-Chih Chou:** State Key Laboratory of Advanced Metallurgy, University of Science and Technology Beijing, Beijing 100083, China. School of Metallurgical and Ecological Engineering, University of Science and Technology Beijing, Beijing 100083, China. E-mail: kcc126@126.com
Jie Dang, Guo-Hua Zhang: State Key Laboratory of Advanced Metallurgy, University of Science and Technology Beijing, Beijing 100083, China. School of Metallurgical and Ecological Engineering, University of Science and Technology Beijing, Beijing 100083, China

to MoO_2 was a one-step process, while above 698 K, an intermediate phase of Mo_4O_{11} could be formed. It was considered that Mo_4O_{11} was formed by the reaction between MoO_3 and MoO_2 other than by reduction of MoO_3 with H_2 (Eqs. (3a), (3b) and (3c)) [4, 15].

$$MoO_3(s) + H_2(g) \rightarrow MoO_2(s) + H_2O(g) \tag{3a}$$

$$3MoO_3(s) + MoO_2(s) \rightarrow Mo_4O_{11}(s) \tag{3b}$$

$$Mo_4O_{11}(s) + 3H_2(g) \rightarrow 4MoO_2(s) + 3H_2O(g) \tag{3c}$$

1.4 Competitive nucleation mechanism

Lalik et al. [16] postulated a competitive nucleation mechanism, which contained at least two parallel routes (Eqs. (4a); (4b) and (4c)) to generate MoO_2.

$$MoO_3(s) + H_2(g) \rightarrow MoO_2(s) + H_2O(g) \tag{4a}$$

$$4MoO_3(s) + H_2(g) \rightarrow Mo_4O_{11}(s) + H_2O(g) \tag{4b}$$

$$Mo_4O_{11}(s) + 3H_2(g) \rightarrow 4MoO_2(s) + 3H_2O(g) \tag{4c}$$

Each rate was highly sensitive to the number of product nuclei present. At first, there were a few nuclei present of either MoO_2 or Mo_4O_{11}, thereby Eqs. (4a) and (4b) would both proceed slowly; once sufficient Mo_4O_{11} nuclei were formed, reaction (4b) would accelerate to dominate the sequence.

1.5 Autocatalytic comproportionation mechanism

An autocatalytic comproportionation mechanism was proposed by Lalik [1] for describing the reduction of MoO_3 to MoO_2. This model is shown as follows:

$$\begin{aligned} &MoO_3(s) + MoO_2(s) + H_2(g) \\ &\quad \rightarrow 2MoO_2(s) + H_2O(g) \quad \text{autocatalytic} \end{aligned} \tag{5a}$$

$$\begin{aligned} &MoO_3(s) + MoO_2(s) \\ &\quad \rightarrow 2MoO_2(s) + 0.5O_2(g) \quad \text{autocatalytic} \end{aligned} \tag{5b}$$

$$4MoO_2(s) + 1.5O_2(g) \rightarrow Mo_4O_{11}(s) \tag{5c}$$

$$Mo_4O_{11}(s) + 3H_2(g) \rightarrow 4MoO_2(s) + 3H_2O(g) \tag{5d}$$

Eq. (5a) represents the topotactic conversion of MoO_3 to MoO_2 and this was accompanied by the vacuum-driven autocatalytic decomposition of MoO_3 (Eq. (5b)). The oxygen released from MoO_3 in the reaction (Eq. (5b)) was recaptured by MoO_2 to generate Mo_4O_{11} (Eq. (5c)). Finally, the accumulated Mo_4O_{11} was reduced by hydrogen back to the MoO_2 as represented by Eq. (5d). Leisegang et al. [17] also studied this reduction process under hydrogen/argon atmosphere (5 vol.% H_2 / 95 vol.% Ar) in situ by means of wide-angle X-ray scattering. The result showed that Mo_4O_{11} phase could be formed probably only in larger crystallites of MoO_3.

The phase transitions and the morphology evolutions during the reduction of MoO_3 to MoO_2 are very important in order to obtain molybdenum powder with good sintering properties [18]. However, there has so far been no detailed paper to report the morphology evolutions during the reduction. Therefore, the objectives of this study are to further elucidate phase transitions and the formation mechanism of Mo_4O_{11} as well as find out the law of morphology evolutions.

2 Materials and experimental procedure

2.1 Materials

Commercially available MoO_3 and MoO_2 powders were used for experiments. The MoO_3 powder was composed of a large number of small grains with an average grain size of 1.279 μm [19]. Mo_4O_{11} was obtained by sintering MoO_3/MoO_2 (molar ratio of 3:1) pellets under Ar gas at

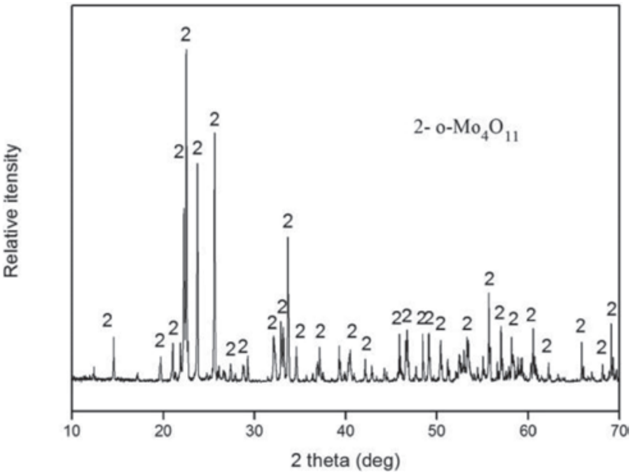

Fig. 1: XRD patterns of Mo_4O_{11} obtained by sintering MoO_3/MoO_2 (molar ratio of 3:1) pellets under Ar gas at a temperature of 833 K for 2 h then at 873 K for 24 h.

833 K for 2 h then at 873 K for 24 h. The X-ray diffraction (XRD) patterns of produced Mo_4O_{11} are shown in Fig. 1.

2.2 Experimental procedure

In order to determine the starting temperature for reducing MoO_3 by hydrogen, the non-isothermal reduction experiment was carried out firstly. The weight change during reduction was monitored by using a thermal analysis system (HCT-2, Beijing Hengjiu Instrument Ltd., China). In the experimental run, the powder of 40 mg was used and filled into an alumina crucible. After the crucible with sample being placed in the furnace, pure hydrogen was introduced into the system to drive air out, and then the furnace was heated from room temperature (around 303 K) to 1273 K with a heating rate of 1 K/min. The weight decrease as a result of the reduction was then monitored continuously. Isothermal reduction experiments were also carried out to study the phase transitions and morphology evolutions. At first samples were heated to the desired reduction temperature with a heating rate of 20 K/min in argon. When the thermal balance was stabilized, the argon was switched to pure hydrogen. After a predetermined period of time, the hydrogen was switched to argon again and the sample was cooled to room temperature.

In all the experiments, a constant flow rate of 0.06 L/min (about 0.318×10^{-2} m/s at room temperature) was kept during the reduction process. Argon used in the experiments was in high purity (<5 ppm O_2). The dew point of H_2 was in the range of 264.5 to 265.4 K (−8.5 to −7.6 °C) and the oxygen content in H_2 was less than 5 ppm. The gas flow rate was controlled by gas flow controllers (Alicant, Model MC-500SCCM-D). Samples were analyzed with XRD (Model, TTRIII, Japan). The morphologies of the samples were observed by Scanning Electron Microscope (SEM, Model S250MK3, Cambridge).

3 Results

3.1 Non-isothermal reduction of MoO_3 powders

The curve of non-isothermal reduction of MoO_3 powders is presented in Fig. 2, from which it can be seen that the reduction of MoO_3 to MoO_2 was started around 671 K, and completed around 810 K. According to the curve slope change, which is increased with the increasing temperature, it can also be obtained that the reduction reaction was accelerated at higher temperature.

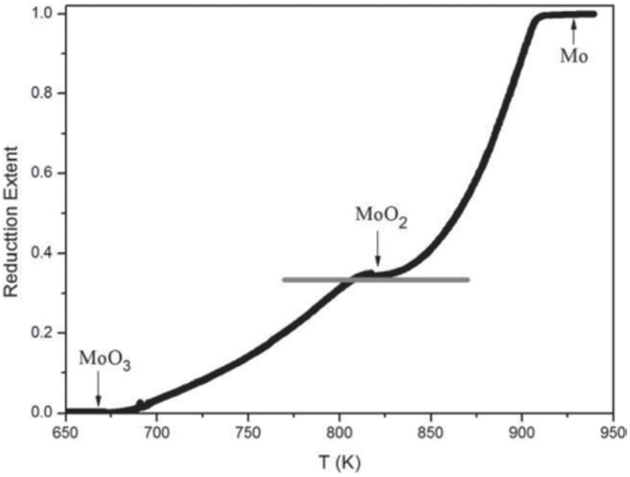

Fig. 2: Non-isothermal reduction curve of MoO_3 powders by pure hydrogen.

3.2 Phase transitions during reduction

The Sample reduced by H_2 for 100 min at 678 K was analyzed by XRD as shown in Fig. 3(a), which indicates that only MoO_2 was formed at this temperature. Fig. 3(b) presents XRD patterns of MoO_3 samples reduced for 160 min at 713 K and 733 K. It can be seen that the peaks of MoO_3, orthorhombic Mo_4O_{11} (o-Mo_4O_{11}) and MoO_2 were all detected, suggesting that o-Mo_4O_{11}, as an intermediate product, presented in the reduction process. Fig. 4 shows XRD patterns of MoO_3 samples (adding 10 mol% Mo_4O_{11} or 10 mol% MoO_2 used for the nucleating agents) reduced for 5 min at 833 K. All the three phases MoO_3, o-Mo_4O_{11} and MoO_2 were detected during the reduction process.

3.3 SEM examinations for morphological analysis

Based on the result of non-isothermal reduction experiment, isothermal reduction experiments in the temperature range from 678 K to 829 K were carried out to study the influence of temperature on the morphologies of generated MoO_2. Fig. 5(a) represents the SEM image of sample reduced at 678 K, which clearly indicates that the majority of generated MoO_2 grains were spherical in shape and the size of grains was considerably large. However, as shown in Fig. 5(b), the morphology of MoO_2 grains changed greatly when the temperature was rising to 713 K. Most of the grains were nearly spherical or oval and the size of grains decreased rapidly though some grains were still large ball-shaped. While Fig. 5(c) indicates that with the temperature reaching 733 K, large MoO_2 grains disap-

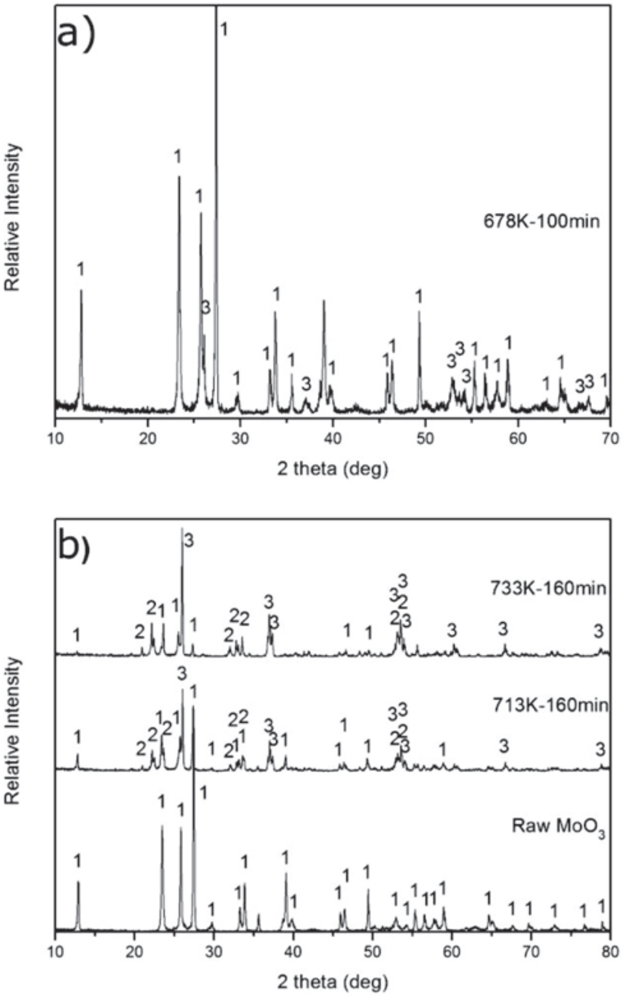

1: MoO_3, 2: o-Mo_4O_{11}, 3:MoO_2

Fig. 3: XRD patterns of MoO_3 samples reduced by pure H_2: a) for 100 min at 678 K; b) for 160 min at 713 K and 733 K.

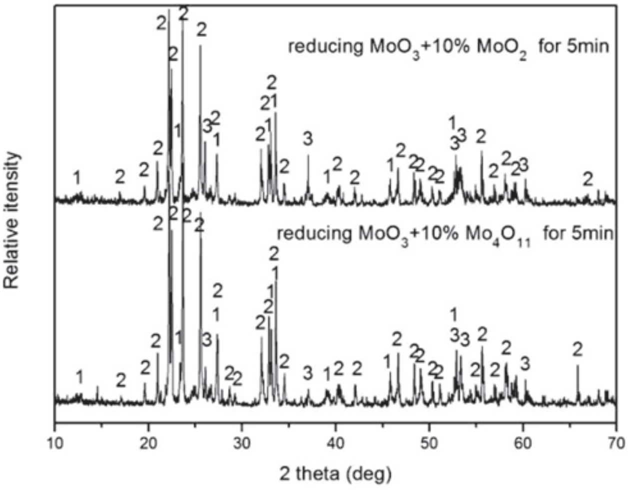

1: MoO_3, 2: o-Mo_4O_{11}, 3:MoO_2

Fig. 4: XRD patterns of MoO_3 samples (adding 10 mol% Mo_4O_{11} and 10 mol% MoO_2) reduced by H_2 for 5 min at 833 K.

peared and meanwhile a small number of plate-shaped MoO_2 grains began forming. At 753 K and 773 K, more plate-shaped MoO_2 grains were formed. When the reduction temperature reached 793 K (Fig. 5(f)), most of MoO_2 grains were plate-shaped. While Fig. 5(g) and Fig. 5(h) indicate that at higher temperature, almost all the MoO_2 grains were large plate-shaped, and the size of these grains is larger than that at 793 K due to the grain growth.

Fig. 6 shows the SEM micrographs of samples after the reduction for different time at 753 K by hydrogen. As shown in Fig. 6(a), the raw MoO_3 powder was nonporous and composed of a number of very small grains. Figs. 6(b) to (e) show the morphology evolutions during the reduction. It can be found that the nuclei were formed on surface of MoO_3 powder then grew to large grains with spherical or oval shape. According to above XRD analysis and the literature report [3], spherical or oval grains should be the intermediate product Mo_4O_{11}. The final product of MoO_2 powder was composed of both small plate-shaped and spherical grains.

4 Discussion

4.1 Formation mechanism of Mo_4O_{11}

XRD results indicated that only MoO_2 was formed during the reduction of MoO_3 at 678 K. While as the temperature reached 713 K and 733 K, o-Mo_4O_{11} was formed. Moreover, the previous work [19] showed that in the temperature range from 755 K to 829 K, the peaks of o-Mo_4O_{11} were also detected in the course of reduction, suggesting the formation of o-Mo_4O_{11} as an intermediate phase at higher temperature. Thus, it can be drawn that at 678 K, the reduction may either be an one-step process, or obey the two-step mechanism, but the rate of reduction of MoO_3 to Mo_4O_{11} was much less than that of Mo_4O_{11} to MoO_2. However, above 713 K, the reduction reaction did not obey the one step mechanism. This result is in accordance with that obtained by Ressler et al. [4].

It has been pointed out that the formation of Mo_4O_{11} owing to the reaction of MoO_3 with MoO_2 in the reduction process of MoO_3 can be neglected [19]. This can be attributed to that the reduction reaction finished in a shorter period comparing with the time for forming Mo_4O_{11} by the reaction of MoO_3 with MoO_2. Hence, under the conditions in the present study, the reduction of MoO_3 did not obey

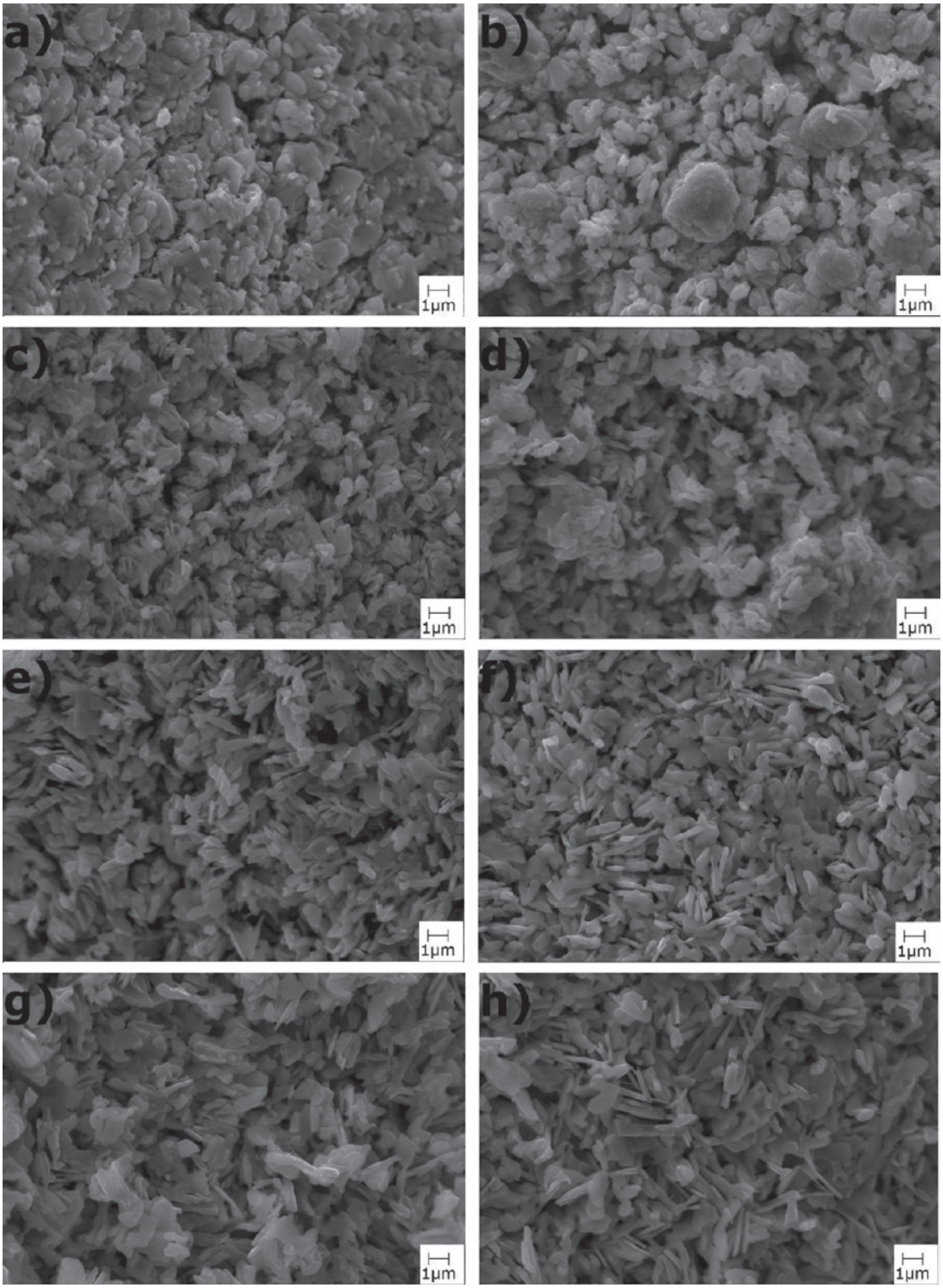

Fig. 5: Morphologies of MoO_3 samples completely reduced by pure H_2 at: a) 678 K; b) 713 K; c) 733 K; d) 753 K; e) 773 K; f) 793 K; g) 813 K; h) 829 K.

the comproportionation mechanism. Taking the results shown in Fig. 4 into account, the competitive nucleation mechanism seemed inadequate to describe the reduction of MoO_3 to MoO_2. According to the competitive nucleation mechanism, $MoO_3 \rightarrow MoO_2$ or $MoO_3 \rightarrow Mo_4O_{11}$ may be very sensitive to nucleation. However, it should be noted that the addition of nucleating agents (10 mol% Mo_4O_{11} or 10 mol% MoO_2) had little influence on the phase transitions

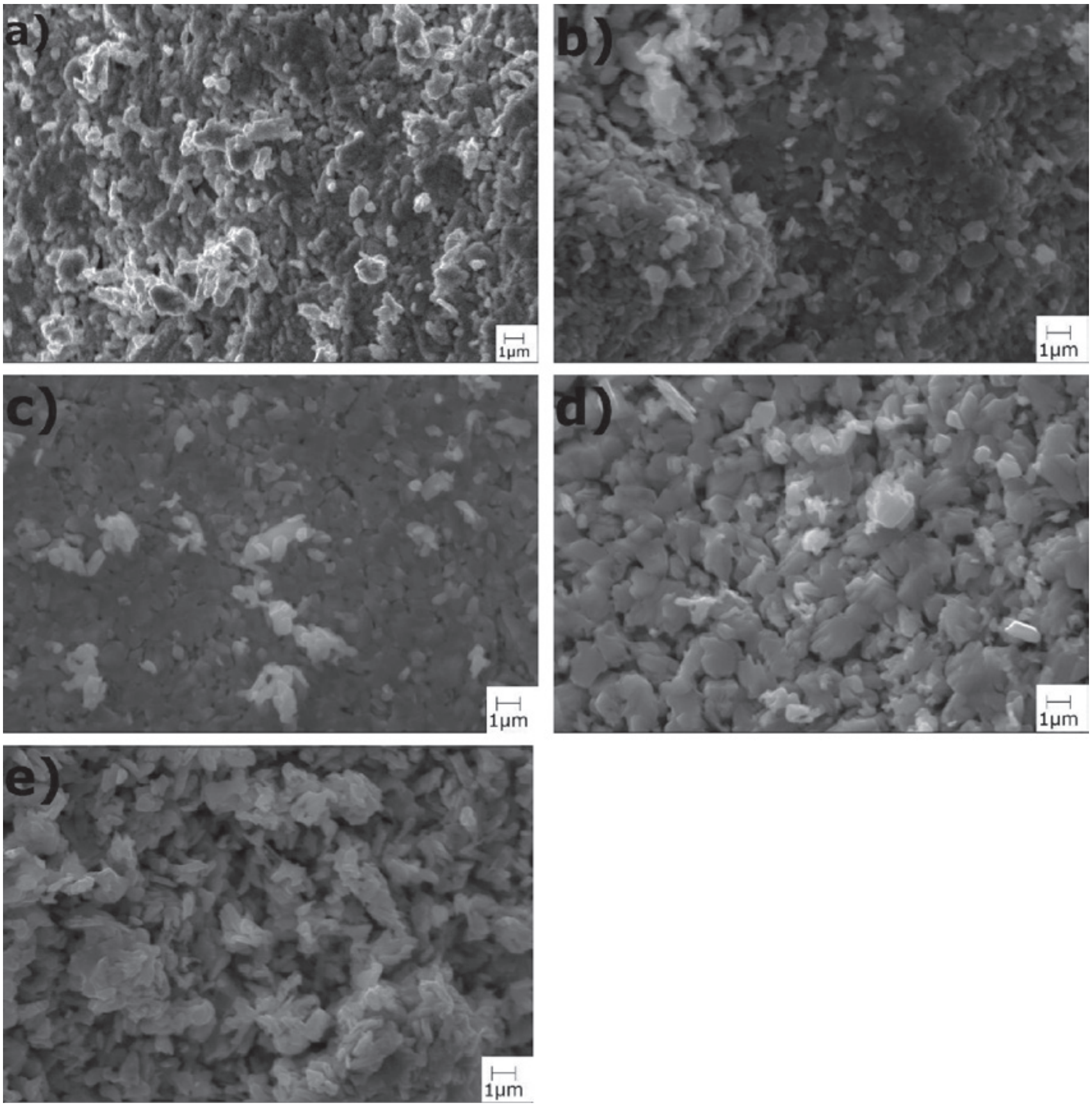

Fig. 6: Morphologies of MoO_3 samples reduced by H_2 at 753 K: a) raw MoO_3; b) reduced for 10 min; c) reduced for 20 min; d) reduced for 60 min; e) completely reduced.

in the reduction course of MoO_3. In addition, Fig. 7 shows the standard reaction Gibbs energy changes for reactions of Eqs. (6) and (7). It can be clearly obtained that O_2 was more likely to react with hydrogen other than MoO_2. Moreover, under the experimental condition of the present study, hydrogen gas was excessive. Therefore, hydrogen would react with oxygen released from MoO_3 in the reaction 5(b) prior to being recaptured by MoO_2.

$$8/3\ MoO_2(s) + O_2(g) = 2/3\ Mo_4O_{11}(s) \tag{6}$$

$$2H_2(g) + O_2(g) = 2H_2O(g) \tag{7}$$

In summary, the formation of o-Mo_4O_{11} during the reduction process of MoO_3 with H_2 is not due to the comproportionation mechanism, competitive nucleation mechanism or autocatalytic comproportionation mechanism but rather due to a two-step reduction mechanism.

4.2 Morphology evolutions

In the present sub-section, the morphology evolutions during the reduction of MoO_3 to MoO_2 at temperature above 713 K will be discussed. It was pointed out in literatures [3, 19] that Mo_4O_{11} and MoO_2 were formed via a chemical vapor transport (CVT) route by gaseous transport phases:

$$MoO_3(s) \rightarrow TP_1(g) \rightarrow Mo_4O_{11}(s) \rightarrow TP_2(g) \rightarrow MoO_2(s) \tag{8}$$

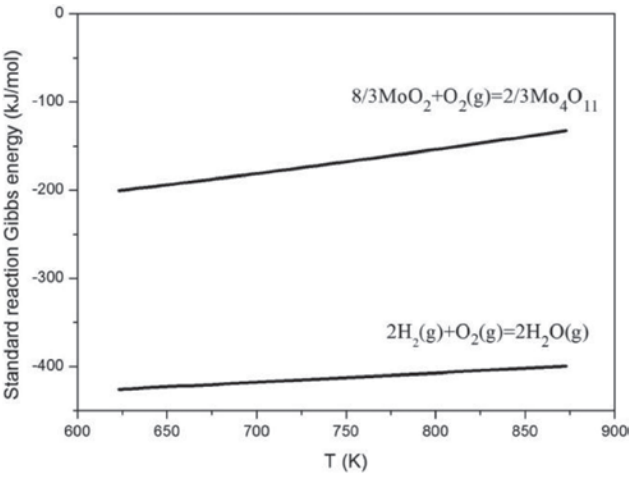

Fig. 7: The standard reaction Gibbs energy as the function of temperature for reactions $8/3MoO_2 + O_2(g) = 2/3Mo_4O_{11}$ and $2H_2(g) + O_2(g) = 2H_2O(g)$

Firstly, the intermediate gaseous transport phase TP_1 was deposited on a nucleus of Mo_4O_{11} and reduced to Mo_4O_{11}. Then the Mo_4O_{11} nuclei formed a grain, and then it grew. With the proceeding of the reduction, a Mo_4O_{11} layer was formed. The stage of reduction of Mo_4O_{11} to MoO_2 was the nucleation of MoO_2 on the surface of Mo_4O_{11} grains with the subsequent growth of MoO_2 grains.

Based on above analysis, the phase transitions and morphology evolutions during hydrogen reduction of MoO_3 to MoO_2 in two temperature ranges, from 713 to 733 K and 753 to 829 K, can be described by the following model presentations.

Fig. 8 shows a mechanism model for the low temperature range from 713 to 733 K. It can be seen that firstly MoO_3 is reduced to large spherical or oval Mo_4O_{11} grains, then to small spherical or oval MoO_2 ones. The mechanism model for the temperature range from 793 to 829 K is

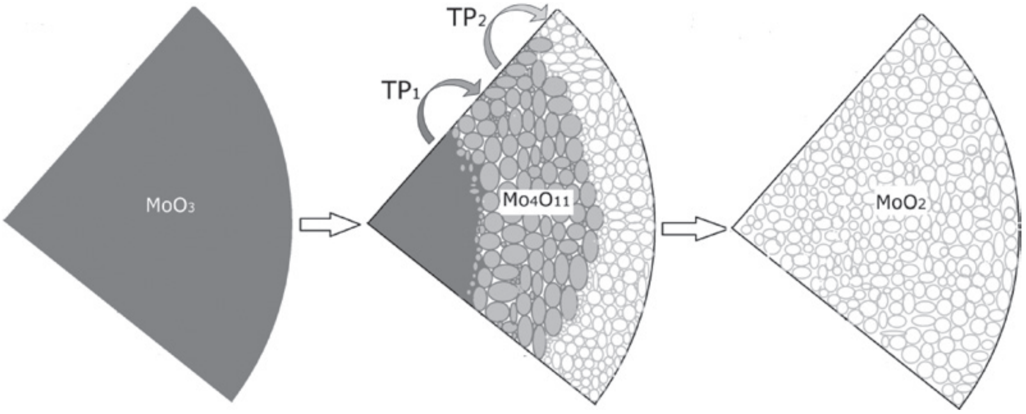

Fig. 8: A model for hydrogen reduction of MoO_3 to MoO_2 at 713 to 733 K.

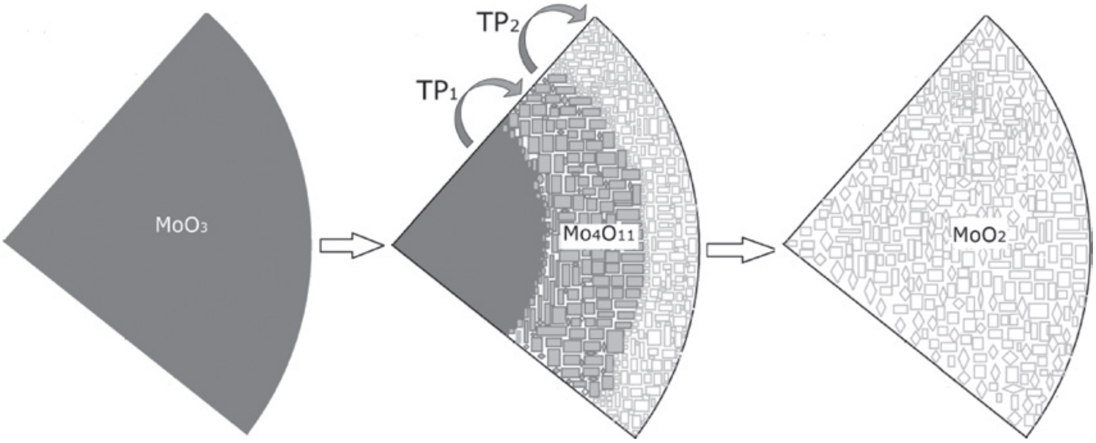

Fig. 9: A model for hydrogen reduction of MoO_3 to MoO_2 at 773 to 829 K.

presented in Fig. 9. MoO_3 is firstly reduced to large plate-shaped but not spherical or oval Mo_4O_{11} grains, then to small plate-shaped MoO_2 ones. The reason for the presence of different morphologies in different reducing temperature ranges may be resulted from the spiral growth mechanism of MoO_2. In this growth manner, the grains grow layer on layer along a specific orientation, which can be obviously seen in Fig. 5. At higher temperature range (793 to 829 K), many molecules of gaseous phases TP_1 and TP_2 can be formed, meanwhile their transport rates can be much faster than those at low temperature (713 to 733 K), thus, more Mo_4O_{11} and MoO_2 nuclei are formed. These nuclei can only grow into plate-shaped grains prior to the completion of the reduction reaction. While from 713 to 733 K, owing to the slow reaction rate and low saturation vapor pressure, the formed Mo_4O_{11} and MoO_2 nuclei are relatively less. There is enough time for the subsequently generated product-nuclei to grow along the thickness direction to form pseudo spherical or oval grains.

5 Conclusions

In the present work, the hydrogen reduction of MoO_3 to MoO_2 in the temperature range of 678 to 829 K was studied. The experiments performed mainly focused on elucidating the phase transitions and the morphology evolutions. The following conclusions can be drawn.

1. At 678 K, no intermediate was observed. While above 713 K, an intermediate product, Mo_4O_{11}, was formed. The formation of Mo_4O_{11} was found to obey the consecutive mechanism instead of other mechanisms.
2. In the temperature range from 713 to 733 K, MoO_3 was firstly reduced to large spherical or oval Mo_4O_{11} grains then to spherical or oval MoO_2 ones. While in the temperature range from 793 to 829 K, most of MoO_3 grains were firstly reduced to large plate-shaped Mo_4O_{11} grains, subsequently to small plate-shaped MoO_2 ones.

The authors would like to acknowledge financial support from the National Natural Science Foundation of China (No. 11220158).

Received: June 30, 2013. Accepted: September 7, 2013.

References

[1] E. Lalik, *Catal. Today*, **169**, (1), 85–92 (2011).
[2] J. Dang, G. H. Zhang and K. C. Chou, *Int. J. Refract. Met. Hard Mater.*, **41**, 356–362 (2013).
[3] W. V. Schulmeyer and H. M. Ortner, *Int. J. Refract. Met. Hard Mater.*, **20**, 261–269 (2002).
[4] T. Ressler, R. E. Jentoft, J. Wienold, M. M. Günter and O. Timpe, *J. Phys. Chem. B*, **104**, 6360–6370 (2000).
[5] J. Orehotsky, L. Jamiolkowski and J. Gerboc, *Mater. Sci. Eng.*, **41**, (2), 237–241 (1979).
[6] P. Arnoldy, J. De Jonge and J. A. Moulijn, *J. Phys. Chem.*, **89**, (21), 4517–4526 (1985).
[7] P. A. Spevack and N. S. McIntyre, *J. Phys. Chem.*, **96**, (22), 9029–9035 (1992).
[8] J. R. Regalbuto and J. W. Ha, *Catal. Lett.*, **29**, (1–2), 189–207 (1994).
[9] L. C. Dufour, O. Bertrand and N. Floquet, *Surf. Sci.*, **147**, (2), 396–412 (1984).
[10] R. Burch, *J. Chem. Soc.*, *Faraday Trans. 1*, **74**, 2982–2990 (1978).
[11] J. Słoczyński and W. Bobinski, *J. Solid State Chem.*, **92**, (2), 436–448 (1991).
[12] J. Słoczyński, *J. Solid State Chem.*, **118**, (1), 84–92 (1995).
[13] J. Słoczyński, *J. Phys. Chem. B*, **106**, (31), 7718 (2002).
[14] J. Słoczyński and W. Bobinski, *J. Solid State Chem.*, **92**, (2), 420–435 (1991).
[15] T. Ressler, R.E. Jentoft, J. Wienold and O. Timpe, *J. Synchrotron Radiat.*, **8**, (2), 683–685 (2001).
[16] E. Lalik, W. I. F. David, P. Barnes and J. F. C. Turner, *J. Phys. Chem. B*, **105**, (38), 9153–9156 (2001).
[17] T. Leisegang, A. A. Levin, J. Walter and D. C. Meyer, *Cryst. Res. Technol.*, **40**, (1–2), 95–105 (2005).
[18] R.K. Enneti and T.A. Wolfe, *Int. J. Refract. Met. Hard Mater.*, **31**, 47–50 (2012).
[19] J. Dang, G. Zhang, K. Chou, R. Reddy, Y. He and Y. Sun, *Int. J. Refract. Met. Hard Mater.*, **41**, 216–223 (2013).